Phylomitogenomics provides new perspectives on the Euphasmatodea radiation (Insecta: Phasmatodea)

Phylomitogenomics provide new perspectives on the Euphasmatodea radiation (Insecta: Phasmatodea).

Giobbe Forni[1], Federico Plazzi[1], Alex Cussigh[1], Oskar Conle[2], Frank Hennemann[3], Andrea Luchetti[1,*] and Barbara Mantovani[1].

[1] Department of Biological, Geological and Environmental Sciences – University of Bologna, via Selmi 3, 40126 Bologna, Italy.

[2] Am Freischütz 14, 47058 Duisburg, Germany.

[3] Tannenwaldallee 53, 61348 Bad Homburg, Germany.

** Corresponding Author: Andrea Luchetti; email: andrea.luchetti@unibo.it*

Giobbe Forni: giobbe.forni2@unibo.it

Federico Plazzi: federico.plazzi@unibo.it

Alex Cussigh: alex.cussigh2@unibo.it

Oskar Conle: conle@phasmatodea.com

Frank Hennemann: hennemann@phasmatodea.com

Andrea Luchetti: andrea.luchetti@unibo.it

Barbara Mantovani: barbara.mantovani@unibo.it

Declarations of interest: none

Forni, et al (2021).Phylomitogenomics provides new perspectives on the Euphasmatodea radiation (Insecta: Phasmatodea). Molecular Phylogenetics and Evolution, 155: 106983 (https://doi.org/10.1016/j.ympev.2020.106983)

Abstract

Phasmatodea species diversity lies almost entirely within its suborder Euphasmatodea, which exhibits a pantropical distribution and is considered to derive from a recent and rapid evolutionary radiation. To shed light on Euphasmatodea origins and diversification, we assembled the mitogenomes of 17 species from transcriptomic sequencing data and analysed them along with 22 already available Phasmatodea mitogenomes and 33 mitogenomes representing most of the Polyneoptera lineages. Maximum Likelihood and Bayesian Inference approaches retrieved consistent topologies, both showing the widespread conflict between phylogenetic approaches and traditional systematics. We performed a divergence time analysis leveraging ten fossil specimens representative of most polyneopteran lineages: the time tree obtained supports an older radiation of the clade with respect to previous hypotheses. Euphasmatodea diversification is inferred to have started ~187 million years ago, suggesting that the Triassic-Jurassic mass extinction and the breakup of Pangea could have contributed to the process. We also investigated Euphasmatodea mitogenomes patterns of dN, dS and dN/dS ratio throughout our time-tree, trying to characterize the selective regime which may have shaped the clade evolution.

Keywords: Divergence time; Evolutionary radiation; Mitogenomics; Phasmatodea.

1. Introduction

Phasmatodea is a a small order of polyneopteran insects, with ~3000 described species present across all major landmasses and with a predominantly tropical distribution. The clades is known to include some of the most outstanding examples of cryptic mimicry, with lineages which resemble leaves, twigs and mosses (Bradler and Buckley, 2018). Several studies are contributing to the understanding of the systematic relationships within this clade, suggesting that present-day distribution is the result of rather recent dispersal events (Simon et al., 2019; Robertson et al., 2018). Nonetheless, many of the hypotheses which have been proposed throughout the years are conflicting. From a morphological perspective, the lack of resolved relationships at deeper nodes can be attributed to the convergent evolution of several morphological features, which blur the boundaries between taxa. At the same time, molecular phylogenetic approaches lack substantial support and consistency for deep relationships, while their outcome is often in disagreement with those found using morphological approaches (Buckley et al., 2010; Bradler et al., 2014; Bradler et al., 2015). Nonetheless, having a solid phylogenetic framework and deciphering the timing of lineages diversification is crucial for our understanding of phasmids evolution and their major adaptations.

The lack of fully resolved relationships in molecular phylogenies can result from a variety of factors, including: (i) uninformative or (ii) conflicting data, (iii) model violations, (iv) high homoplasy and (v) incomplete lineage sorting. A possible biological explanation for weak phylogenetic signal may also lie in ancient and rapid radiations (Whitfield et al., 2007), which are often associated to low supports at deeper nodes and the lack of consistency when different kind of data and analytical approaches are employed. This uncertainty can sometimes be resolved by either increasing the amount of data or by having a more extensive taxon sampling (Bragg et al., 2018).

Several processes can be involved in radiations, including a wide range of biotic and abiotic factors (Simões et al., 2016). Adaptive radiations can be triggered by key evolutionary innovations and/or exaptation. This has been proposed, for example, for the antifreeze glycoproteins of notothenioid fishes living in the ice-cold waters of Antarctica (Matschiner et al., 2011) or for wing patterns, pollen feeding and the expansion of olfactory receptor gene families that are related to a burst of diversification in *Heliconius* butterflies (Kozak et al., 2015). On the other hand, the increase in diversifications within a clade can also be driven by a wide range of abiotic factors which affect physical isolation, such as climate shifts or physical barriers (Lopèz-Estrada et al., 2018). Evolutionary radiations can also occur concurrently across different clades, as described by the Turnover-Pulse theory, which postulates that physical changes trigger biotic changes eventually resulting in a process of lineages turnover across a wide range of clades (Vrba, 1993).

We aimed to investigate the processes that shaped the initial divergence of Euhasmatodea lineages using mitochondrial genomes, which are an increasingly common tool for molecular systematics and phylogenetics in metazoan, particularly in insects (Cameron, 2014). Their wide use stems from the ease of getting new sequence data for a set of clearly orthologous genes, which can be readily compared to an increasing amount of available mitogenomic sequences. Mitogenomes have been used many times to solve controversial systematic relationships at inter-ordinal (Rota-Stabelli and Telford, 2008; Song et al., 2016; Rutschmann et al., 2017) or intra-ordinal (Bourguignon et al., 2018; Li et al., 2017; Timmermans et al., 2014) taxonomic levels.

Although sequence variation in mitochondrial DNA was traditionally considered selectively neutral (Dowling et al., 2008), there is an increasing evidence that mitogenomes can experience episodes of positive selection as a consequence of shifts in physiological or environmental conditions. Those modifications underlie metabolic adaptations such as the accommodation of hematophagy and the origin of flight in vampire bats (Botero-Castro et

al., 2018; Shen et al., 2010), lung reduction and venom evolution in snakes (Castoe et al., 2008), or the evolution of bioelectrogenesis in fishes (Elbassiouny et al., 2019). Also environmental conditions may affect mitochondrial genomes evolution, as pointed out in several animal taxa like marine and terrestrial mammals (Hassanin et al., 2009; Foote et al., 2011; Tomasco and Lessa, 2011), birds (Zhou et al., 2014), fishes (Wang et al., 2016), bivalve molluscs (Plazzi et al., 2017) and hexapods (Jiang et al., 2018; Yuan et al., 2018; Carapelli et al., 2019).

In the present paper we reconstructed new mitogenome sequences for 17 phasmid species from transcriptomic data deposited in the NCBI SRA database and analysed them in a wide phylogenetic framework along with previously published data of phasmid and other representatives of the major polyneopteran orders. Our aim was to investigate the evolutionary radiation of its suborder Euphasmatodea: we leveraged several well characterized fossils - mainly external to the Phasmatodea clade - to perform a divergence time analysis and obtained a timeframe for phasmid evolution which is found older from previous estimates. Moreover, we investigated the possibility of selective pressures which may have shaped the mitogenomes genetic variation.

2. Materials and Methods

2.1. Mitogenomes assembly and annotation.

We downloaded the RNA-Seq reads of all the 17 euphasmatodean species which did not have a corresponding mitogenome already assembled (last checked in March 2019) (Table 1). Reads were quality trimmed with a phred score threshold of 33, with a 25 bp-sliding window using Trimmomatic (Bolger et al., 2014) and quality checked with FastQC (Andrews, 2010). The Python script mitoRNA was then used to assemble mitogenomes from transcriptomic data (Forni et al., 2019; available at https://github.com/mozoo/MitoRNA): this consists of a target assembly process, based on an iterative reference

mapping and de-novo assembly process. This straightforward approach is useful to recover mitochondrial genomes from RNA-Seq experiments, given a reference. For each transcriptome analysed, all available phasmid mitogenomes (last checked in March 2019) were used as starting references for mitoRNA. On the obtained contigs, the 13 protein coding genes (PCGs) and the two ribosomal RNA (rRNAs) genes were manually annotated, following the closest reference sequence. Control regions and tRNAs where omitted as they presented a low coverage, due to the transcriptional architecture of mitochondria (Forni et al., 2019).

2.2. Dataset, saturation and base composition analyses.

We carried out phylogenetic analyses on the newly obtained 17 nearly complete molecules combined with the 22 mitogenomes already available for Euphasmatodea (Table 1), bringing the total number up to 39. Additionally, we included 35 Polyneoptera mitogenomes for tree rooting and time tree calibration (Suppl. Table S1). We excluded representatives from the two orders Zoraptera and Embioptera due to phylogenetic artefacts, especially long branch attraction, that those mitogenomes are known to generate (Song et al., 2016).

Each gene was separately aligned using MAFFT with the option *--auto* for PCGs and *X-INS-i* for rRNAs (Katoh et al., 2013). PCG alignments were also inspected using AliView (Larsson, 2014) to select the correct reading frame and to check for stop codons. All poorly aligned regions were removed using Gblocks, v.0.91b (Castresana, 2000) with default settings and the codon parameter. Saturation and composition analyses were then performed using DAMBE v. 7.0.28 (Xia, 2018) on each single gene and on the concatenated alignment, with and without the third codon position. Saturation analyses were also carried out on a subset including only the Phasmatodea spp. We also used

Aligroove to test for data heterogeneity on the concatenated alignment, with and without the third codon position.

Alignments, including the sequences of annotated genes of the new 17 mitochondrial genomes generated in this study, were deposited in Figshare (doi: https://doi.org/10.6084/m9.figshare.9885176.v3). The final concatenation was partitioned into three subsets: (i) first codon positions of PCGs; (ii) second codon positions of PCGs; (iii) small and large ribosomal subunit rRNAs.

2.3. Model selection, phylogenetic inference and divergence time analysis.

Model selection, Bayesian Inference and Maximum Likelihood analyses were carried out through the CIPRES Science Gateway (www.phylo.org).

For Bayesian Inference, the best-fit nucleotide substitution model and the optimal partitioning scheme were determined using PartitionFinder2, based on the corrected Akaike Information Criterion (Suppl. Table S2; Lanfear et al., 2016). The concatenated sequence alignment was analysed using BEAST 2.4.8 (Bouckaert et al., 2014) jointly estimating topology and node age. An uncorrelated lognormal relaxed clock model of rate variation across branches was implemented as a time prior and both Yule and Birth-Death speciation processes were used for the tree prior. Node calibrations were set using 10 fossil taxa with justified phylogenetic placement (Table 2). The minimum age constraints based on fossil records were implemented as exponential priors, with soft maximum priors (95% probability) taken from Bourguignon et al., 2018 or fixed at 411 Million years ago (Mya), which is the estimated age of the oldest hexapod fossil (*Rhyniella praecursor* Hirst & Maulik, 1926; Wolfe et al., 2016). Four replicates of the MCMC analysis were run with trees and parameter values sampled every 5,000 steps over a total of 700 million generations. A 10% burn-in was discarded and the estimated sample size of parameters

were assessed (ESS>200) using Tracer 1.6 (Rambaut et al., 2018). Run convergence was estimated with Tracer 1.6 and by visually comparing tree topologies.

In order to test the reliability of our inferred topology, we also analysed the concatenated sequence alignment of nucleotides and amino acids using the Maximum Likelihood approach of IQ-TREE v1.6.1 (Trifinopoulos et al., 2016). The best-fit models of nucleotide substitution were identified using IQ-TREE Model Selection (Suppl. Tab. S4; Kalyaanamoorthy et al., 2017) using the FreeRate model and the edge-linked parameter. Ten ML searches were run with 1,000 ultrafast bootstraps replicates; the run with the best likelihood was selected as the most reliable.

We downloaded all fossil occurrences of arthropods from the Fossilworks database (http://fossilworks.org) and generated three-timer (3T) origination and extinction rates, which were plotted through time. These metrics implement a sliding window approach, which is considered to minimize the artefacts deriving from the variation in sampling completeness (Alroy et al., 2008).

2.4. dN/dS analysis

The dN, dS and dN/dS ratios for each gene and for the concatenated matrix were calculated using the branch model of the CODEML program implemented in PAML 4.8a (Yang, 2007). The IQ-TREE-computed tree with fixed branch lengths was set as the user tree. Two models were used for dN/dS estimation: i) a single dN/dS ratio along the entire tree (model 0); ii) a specific dN/dS ratio for each given branch in the tree (model 1). We then used the likelihood ratio test (LRT) to determine the best-fitting model (Yang et al., 2007). Before all subsequent analyses, we excluded dN/dS estimates derived from values of dS<0.01, as they could lead to biased dN/dS estimates, as well as values of dN>2 and dS>2, which could indicate saturation of substitutions (Villanueva-Cañas et al., 2013). The timespan covered by the inferred time-tree was split into time bins of 10 million years and

for each one we gathered the median of dN/dS values relative to all contemporary branches, for each PCG and their concatenation (as described in Plazzi et al., 2017). To check for possible biases in our analyses on selective pressures, linear regression were carried out a) between median dN, dS, dN/dS values and temporal midpoint of each time bin in the complete time-tree, b) between median dN, dS, dN/dS values and temporal midpoint of each time bin in the Phasmatodea sub-tree, c) between dN, dS, dN/dS values and the branch lengths found in the Maximum Likelihood inference, d) between dN, dS and dN/dS. We also tested for significant differences in dN, dS and dN/dS ratio between the branch leading to *Timema californicum* Scudder, 1895 and the one leading to Euphasmatodea by means of the two-tailed Wilcoxon signed rank test.

3. Results

3.1. Dataset, saturation and base composition analyses

When analyzed using Xia's method, all alignments showed little to no saturation (ISS < ISS.C; P<0.001), but ISS values were found smaller when the 3rd codon positions were excluded from PCGs (Suppl. Table S3a). The same method was applied to the sequences of phasmatodean species only, giving similar results as for the complete dataset (Suppl. Table S3b). When considering only the third codon positions of PCGs, the majority of the genes showed signs of saturation in the complete dataset, while it was present to a lesser extent when only phasmid species were considered (Suppl. Table S3c). Several genes and the concatenated alignment were found to have a heterogeneous nucleotide composition, even when excluding third codon positions (Chi-square test, P<0.01; Suppl. Table S4). However, values of Cramer's V, which measure the strength of the observed heterogeneity (i.e. the strength of association between nucleotide composition and taxa in the Chi-square test; Cramer, 1946), were low (<0.15), and were even lower when excluding 3rd codon positions. This, therefore, suggested that the observed nucleotide

frequency differences among the taxa was not expected to substantially affect the phylogenetic inference under time-reversible models of evolution. Moreover, AliGROOVE showed a general lack of confounding signals related to sequence heterogeneity (Suppl. Fig. S1). Phylogenetic inferences were performed on a final matrix which included 72 species and 13,547 nucleotide positions, resulting from the concatenation of all the genes after the use of GBlocks and the removal of the 3rd codon position from PCGs.

3.2. Mitochondrial phylogeny and divergence times

Maximum Likelihood (-*lnL* = -215066.9305) analysis and Bayesian inferences, using both the Birth-Death (-*lnL* = -215655.2673) and Yule (*lnL* = -215655.8712) tree priors, produced identical topologies (Fig. 1; Fig. 2; Suppl. Fig. S2A-C). Since no Embioptera mitogenome was included in the analysis due to the phylogenetic artefacts associated to them (Song et al., 2016), the Notoptera clade (which includes the two orders Grylloblattodea and Mantophasmatodea) was recovered as phasmids sister lineage. Within the Phasmatodea clade, the first split was represented by the divergence between *Timema californicum* Scudder, 1895 (Timematodea) and the highly supported, monophyletic clade of Euphasmatodea (posterior probability, PP=1.0; bootstrap proportion, BP=100). While a few euphasmatodean families, like Phylliidae, formed highly supported clades, most of the families appeared either paraphyletic (Diapheromeridae) or polyphyletic (Phasmatidae and Lonchodidae). At the subfamily level, the supported clades were Phylliinae (*Phyllium giganteum* Hausleithner, 1984, *Ph. tibetense* Liu, 1993 and *Ph. siccifolium* (Linné, 1758)) (PP=1, BP=100), Necrosciinae (*Micadina phluctainoides* (Rehn, 1904), *Neohirasea japonica* (Haan, 1842), *Sipyloidea sipylus* (Westwood, 1859) and *Calvisia medogensis* Bi, 1993) (PP=1, BP=100) and Lonchodinae (*Phraortes elongatus* (Thunberg, 1815) [= *illepidus* Brunner v. Wattenwyl, 1907], 1907, *Phraortes* sp. Iriomote Island, *Phraortes* sp. Miyako Island, *Carausius morosus* (Sinéty, 1901), *Megalophasma granulatum* Bi, 1995)

(PP=1, BP=100). It has to be noted, though, that another available *Phraortes* sp. sample do not cluster with the other *Phraortes* species; no information is available about the specimen voucher and it could be likely a species misidentification. While several genera, like *Micrarchus* Carl, 1913, *Bacillus* Berthold, 1827, *Phraortes* Stål, 1875 and *Phyllium* Illiger, 1789 were recovered as monophyletic, *Ramulus* Saussure, 1862 was found paraphyletic and *Tectarchus* Salmon, 1954 appeared polyphyletic. As defined by Buckley et al. (2010), the New Zealand clade (labelled in Fig. 2) was here confirmed as monophyletic, with maximum support (PP=1, BP=100). The ML inference on the amino acid dataset (*-lnL* = -131128.4724) presented a slightly different topology regarding the Euphasmatodea clade with respect to the ML and BI inferences based on the nucleotide dataset. However, when collapsing poorly supported branches (BP<85) the two trees are fully compatible (Suppl. Fig. S2).

Divergence time estimates (Fig. 2) indicated that Phasmatodea diversification dates back to the Mid-Permian, 273.8 million years ago (95% HPD = 233.4-320.6 Mya), when the divergence between the *Timema* lineage and the Euphasmatodea clade took place. The Euphasmatodea radiation started in the Mid-Jurassic (187.5 Mya; 95% HPD = 145.3-205.8 Mya) and by the End Jurassic-Early Cretaceous all family-level lineages were already established. The New Zealand clade would have diverged later, the estimated age being 71.3 Mya (95% HPD = 53.8-89.5 Mya).

3.3. dN/dS analysis

For all single genes and the concatenated dataset, the null hypothesis that a single dN/dS applies to all the tree branches was rejected by the LRT test (P<0.001; Suppl. Table S5) and the alternative hypothesis of a dN/dS value for each branch was, therefore, accepted.

We found that dN/dS ratios showed a significantly positive correlation with time, both with the complete dataset and with the Phasmatodea sub-tree only (Fig. 3; Suppl. Fig. S3A-3B). To tentatively check whether these dN/dS estimates might have resulted from biased dN or dS values, although potentially problematic values were already filtered out (Villanueva-Cañas et al., 2013), we investigated their possible dependency from time and branch length. Both dN and dS values do not correlate with time in the complete dataset or correlate negatively in the Phasmatodea sub-tree only (Suppl. Fig. S3A-3B). Moreover, as expected, dN and dS correlated significantly with branch lengths, while dN/dS do not (Suppl. Fig. S3C). Finally, no correlation was found between dS and dN/dS both in the complete dataset and when considering only the Phasmatodea sub-tree (Suppl. Fig. S3D). Interestingly, values of dN, dS and dN/dS calculated over the 13 PCGs for the *T. californicum* and Euphasmatodea stem branches resulted significantly different (Wilcoxon signed ranked test, $P<0.001$) (Table 3). Overall, comparing dN/dS values between the two branches, the difference varies between 1.4-fold to 8.6-fold, depending on the gene considered (Table 3).

4. Discussion

4.1 Relationships among Euphasmatodea lineages

New mitochondrial DNA data have been recovered for 17 phasmid species, by mining transcriptome sequencing, and are analysed in a phylomitogenomic framework for the first time. Overall, our analysis includes representative of eight out of the ten recognised polyneopteran orders and six Euphasmatodea families out of the eleven described. In our analysis, the systematic relationships of the polyneopteran orders are congruent with previous findings based on both molecular markers and phylogenomics with either mitochondrial (Song et al., 2016) or nuclear genes (Misof et al., 2014). The placement of all the euphasmatodean species included in the analysis and the relationships between

families and subfamilies are generally consistent with previous phylogenetic analysis on this clade both using whole mitogenomes (Kômoto et al., 2010; Zhou et al., 2017) and molecular markers (Tilgner, 2002; Whiting et al., 2003; Bradler, 2009; Kômoto et al., 2011; Bradler et al., 2014). Despite recently proposed as a new family (Robertson et al., 2018), being supported also by different studies (Bradler et al., 2014; Bradler et al., 2015; Goldberg et al., 2015), we recovered Lonchodidae as a polyphyletic group, consistently with other analyses that utilized mitogenomes (Kômoto et al., 2011; Zhou et al., 2017) and molecular markers (Buckley et al., 2010; Glaw et al., 2019). In our analysis *Megacrania alpheus* (Westwood, 1859) and *Phobaeticus serratipes* (Gray, 1835), both belonging to the family Phasmatidae, form a monophyletic cluster, consistently with Kômoto et al. (2011). On the contrary, in Zhou et al. (2017), *M. alpheus* was instead recovered as the sister taxon of *Extatosoma tiaratum* (Macleay, 1826) and *Phobaeticus serratipes*. The Necrosciinae clade presents a topology consistent with previous works dealing with the same species (Kômoto et al., 2011; Zhou et al., 2017) and the placement of *Neohirasea japonica* in this clade validates the change of the taxonomic status from Lonchodinae to Necrosciinae suggested by Bradler et al. (2014). The New Zealand clade presents a topology largely consistent with the previous literature based on molecular markers; the only difference we found in our inferred topology is that while in the previous literature (Trewick et al., 2008; Buckley et al., 2010; Bradler et al., 2015; Dennis et al., 2015) *Niveaphasma annulatum* (Hutton, 1898) was in a sister relationship with *Micrarchus hystriculeus* (Westwood, 1859) and *Asteliaphasma jucundum* (Salmon, 1991) was external to this group, in our work we recover a sister relationship between *Asteliaphasma jucundum* and *Niveaphasma annulatum*, and *Micrarchus hystriculeus* clustered with the congeneric *Mirarchus* spp. (PP=1, BP=100).

4.2 Timing of Euphasmatodea evolution

In order to provide a temporal framework for the evolution of phasmids, we calculated a time tree using fossils calibration. Fossil calibrations on phasmids have been already used in previous studies, recovering the origin of Phasmatodea between 90 and 122 Mya and the one of Euphasmatodea between 50 and 61 Mya ago (Buckley et al., 2010; Bradler et al. 2015; Robertson et al., 2018, Simon et al., 2019). However, as acknowledged by the same authors, the use of those fossil calibrations could have potentially led to a substantial underestimation of cladogenetic events (Buckley et al., 2010; Bradler et al., 2015). Therefore, in order to avoid such a possible bias, we included calibration points based on eight polyneopteran fossils and only two phasmid fossils. Our analysis dates the appearance of major Polyneoptera orders consistently with previous studies which used molecular markers, mitogenomics and nuclear phylogenomics (Misof et al., 2014; Tong et al., 2015; Legendre et al., 2105; Bourguignon et al., 2018, Evangelista et al., 2019; Montagna et al., 2019) (Suppl. Fig. S4). In our time tree, the Phasmatodea clade is estimated ~275 Million years old and the Euphasmatodea crown group is dated shortly after 190 Mya: these dates are somehow consistent with estimates obtained in recent phylogenetic analyses based on whole mitogenomes (Bourguignon et al., 2018) and transcriptomes (Evangelista et al., 2019). Our results are also congruent with the literature on phasmids fossils: a recent paper by Yang et al. (2019) provides support for a diversification of major clades of stick insects happening during or before the mid-Cretaceous. Moreover, the presently obtained estimates of Phasmatodea origin are consistent with the oldest fossils attributed to this taxon, such as *Arachnophasma scurra* (279.5-272.5 Mya; Aristov and Rasnitsyn, 2015) or *Isadyphasma bashkuevi* (259-254 Mya; Gorochov et al., 2013) which were not used as calibrations points for the divergence time analysis.

The outcome of our dating analysis suggests that, the radiation of Euphasmatodea most likely occurred shortly after the Triassic-Jurassic boundary (~200 Mya). There are mainly

two events that could have played key roles in the evolutionary radiation and diversification of this order of insects: the concurrent mass extinction event and the beginning of the Pangea break up.

The coincidence of the Euphasmatodea radiation and the breakup of Pangea which started around 180 Mya (McIntyre et al., 2017) supports a diversification scenario where vicariance has contributed significantly to shape phasmid distribution and diversity. Yet, instances of long-range dispersal, cannot be ruled out: for example, it has been shown that eggs of *Megacrania tsudai* Shiraki, 1933 can be dispersed by floating on the marine surface (Kobayashi et al., 2014) and those of *Ramulus mikado* (Rehn, 1904) can be dispersed by birds (Suetsugu et al., 2018, where it is referred to as *Ramulus irregulariterdentatus*). However, it is still unclear whether passive, long-range dispersal capacities are common among stick insects and they probably cannot be generalized at the level of the entire order. Previous hypotheses on the divergence of New Zealand phasmids dated the event at 26 Mya (16.8 – 35.5 Mya; Buckley et al. 2010), supporting a long-range dispersal from New Caledonia subsequent to the putative re-emergence of New Zealand (22 Mya). On the contrary, our divergence time estimate for the clade is retrieved at 73 Mya (95% HPD = 54.8 – 91.7 Mya), which is consistent with a vicariance scenario and a long-term survival of phasmatodean lineages in New Zealand.

The ecological modifications and the increase in habitat diversity associated with the Pangea fragmentation have been linked to an increase of metazoan diversity (Jordan et al., 2016) and could have played a key role in the diversification of other polyneopteran (Svenson, et al., 2009) and non-polyneopteran (Tang, et al., 2019) insect clades. Environmental perturbations, such as the Triassic-Jurassic extinction, have been also associated with high lineage turnover in different clades, such as amphibians (Roelants et al., 2007), reptiles (Toljagic et al., 2013) and insects as well (Tang et al., 2019). This turnover dynamic can be also observed for most arthropods, indicating a phenomenon that

affected several clades at the same time (Fig. 3). Having found Euphasmatodea radiation shortly after the Triassic-Jurassic boundary suggests that their diversification could have happened in the context of a wider process of lineages turnover.

4.3 Molecular evolution of Euphasmatodea mitogenomes

We investigated dN/dS ratios throughout the inferred time-tree in order to better understand the evolution of euphasmatodean mitogenomes. The dN/dS ratio is widely used to infer changes in selection regimes, but it is known that its estimation can be affected by substitution saturation, which may result in an underestimation of the real number of synonymous substitutions and eventually leading to inflated dN/dS values. We tried to correct estimates for saturation by excluding values of of dN and dS >2, as they may actually imply undetected multiple substitutions (Villanueva-Cañas et al., 2013). Moreover, specific tests indicated that saturation is a marginal feature of our dataset, being only observed in some genes 3rd codon positions. We further analyzed the dN and dS behaviour with respect to time, branch length and dN/dS, in order to have a better understanding of possible biases. First of all, both dN and dS showed the same trend when correlated with time, suggesting that both are similarly affected. Second, dS values well correlated with branch length, indicating that longer branches do not lead to dS underestimation. Third, dN/dS values do not correlate with dS, implying that higher dN/dS values are not resulting by low, potentially underestimated dS values. Overall, these results suggested that obtained dN/dS values are reliable.

Two observations are worth to be considered, that may have implications with phasmid evolution: 1) Euphasmatodea stem branch presented significantly higher dN/dS values compared to the stem branch of *T. californicum*; 2) higher dN/dS values were found in the early-diverging branches of the Phasmatodea sub-tree compared to the more recent ones.

The difference observed between euphasmatodean and *T. californicum* stem branches is difficult to explain, although we may speculate about possible adaptive processes acting on mitogenomes. In fact, a generalized reduction of selective pressures should impact similarly all the molecule, the observed differential pattern across genes is expected in case of an adaptive process (Tomasco and Lessa, 2011). However, it is interesting to note that branches with higher dN/dS values were those corresponding to early divergences: this may indicate a possible implication in the subsequent euphasmatodean radiation. It is, therefore, possible to hypothesize that a relaxation of selective pressures may have helped during the early steps of the radiation, when environmental condition changed because of the Pangea fragmentation, eventually facilitating phasmid diversification. This is, in fact, consistent with the lower dN/dS value of *T. californicum* stem branch, and the limited diversity and restricted geographic distribution of Timematodea species (Vickery and Sandoval, 2001). Alternatively, it can be considered that a rapid radiation may have concurred to shape dN/dS values: it is known in fact, that mildly deleterious, non-synonymous mutations can be randomly brought to fixation as a consequence of low effective population size (Ne) and the subsequent relaxation of purifying selection (Otha, 1993; Woolfit and Bromhan, 2005; Hughes 2007; Brandvain and Wright, 2016). A decrease in Ne can be caused by the occurrences of narrow and repeated colonization bottlenecks which happen during a radiation. When main lineages emerged and the radiation process slowed down a purifying selection regime was restored. However, this cannot explain the higher dN/dS value on the Euphasmatodea stem branch occurring before the radiation.

Conclusions

Mitogenomics provided a novel perspective on Euphasmatodea diversification. Our analyses supported a more ancient radiation of Euphasmatodea than previously thought:

this new perspective suggested several contemporary events which could have acted as drivers of the clade fast diversification. Euphasmatodea radiation appeared coincident with the Pangea fragmentation and, therefore, vicariance could have played a prominent role in shaping the diversity and distribution of leaf and stick insects. Their diversification, then, could have taken place in the context of a wider dynamic of lineages turnover that occurred subsequently to the Triassic-Jurassic mass extinction. Our analyses also suggested that a possible relaxation of selective pressures may have played a role in facilitating the Euphasmatodea radiation.

Acknowledgements

The present work has been supported by Canziani funding to AL and BM. We wish to thank the two anonymous Reviewers and the Editors for their useful and constructive comments that greatly improved the manuscript.

5. References

Alroy J. 2008. Dynamics of origination and extinction in the marine fossil record. Proc. Natl. Acad. Sci. USA. 105, 11536–11542.

Andrews, S. 2010. FastQC. http://www.bioinformatics.babraham.ac.uk/ projects/fastqc/.

Aristov, D.S. and Rasnitsyn, A.P. 2015. New insects from the Kungurian of Tshekarda fossil site in Permian territory of Russia. Russian Entomol. J. 24:17-35

Bethoux, O., Nel, A., Lapeyrie, J., Gand, G., Galtier, J. 2002. *Raphogla rubra* gen. n., sp. n., the oldest representative of the clade of modern Ensifera (Orthoptera: Tettigoniidae, Gryllidea). Eur. J. Entomol. 99, 111–116.

Bolger, A.M., Lohse, M., Usadel, B. 2014. Trimmomatic: a flexible trimmer for Illumina sequence data. Bioinformatics 30, 2114–2120.

Botero-Castro, F., Tilak, M.K., Justy, F., Catzeflis, F., Delsuc, F., Douzery, E.J.P. 2018. In cold blood: compositional bias and positive selection drive the high evolutionary rate of vampire bats mitochondrial genomes. Genome Biol. Evol. 10, 2218-2239.

Bouckaert, R., Heled, J., Kühnert, D., Vaughan, T., Wu, C-H., Xie, D., Suchard, MA., Rambaut, A., Drummond, A. J. 2014. BEAST 2: A Software Platform for Bayesian Evolutionary Analysis. PloS Comput. Biol., 10, e1003537.

Bourguignon, T., Tang, Q., Ho, S.Y.W., Juna, F., Wang, Z., Arab, D. A., et al. 2018. Transoceanic dispersal and plate tectonics shaped global cockroach distributions: evidence from mitochondrial phylogenomics. Mol. Biol. Evol. 35, 970–983.

Bradler, S., 2009. Die Phylogenie der Stab-und Gespenstschrecken (Insecta: Phasmatodea), Thesis, University of Göttingen.

Bradler, S., Buckley, T. R. 2018. Biodiversity of phasmatodea. Insect Biodiversity: Science and Society, 2, 281-313.

Bradler, S., Robertson, J.A., Whiting, M.F. 2014. A molecular phylogeny of Phasmatodea with emphasis on Necrosciinae, the most species rich subfamily of stick insects. Syst. Entomol. 39, 205-222.

Bradler, S., Cliquennois, N., Buckley, T.R. 2015. Single origin of the Mascarene stick insects: ancient radiation on sunken islands? BMC Evol. Biol. 15, 196.

Bragg, J.G., Potter, S., Silva, A.C.A., Hoskin, C.J., Bai, B.Y.H., Moritz, C. 2018. Phylogenomics of a rapid radiation: the Australian rainbow skinks. BMC Evol. Biol. 18, 1–12.

Brandvain, Y., Wright, S.I. 2016. The limits of natural selection in a nonequilibrium world. Trends Genet. 32, 201–210.

Brongniart, C. 1885. Les Insectes fossiles des terrains primaires: coup d'oeil rapide sur la faune entomologique des terrains paléozoïques. Rouen,impr. J. Lecerf.

Buckley, T.R, Attanayake, D., Nylander, J.A.A., Bradler, S. 2010: The phylogenetic placement and biogeographical origins of the New Zealand stick insects (Phasmatodea). Syst. Entomol. 35, 207-225.

Cameron, S.L. 2014. insect mitochondrial genomics: implications for evolution and phylogeny. Annu. Rev. Entomol. 59, 95–117.

Carapelli, A., Fanciulli, P.P., Frati, F., Leo, C., 2019. Mitogenomic data to study the taxonomy of Antarctic springtail species (Hexapoda: Collembola) and their adaptation to extreme environments. Polar Biol. 42, 715–732.

Castoe, T.A., Jiang, Z.J., Gu, W., Wang, Z.O., Pollock, D.D., 2008. Adaptive evolution and functional redesign of core metabolic proteins in snakes. PLoS ONE. 3, e2201–2214.

Castresana, J. 2000. Selection of conserved blocks from multiple alignments for their use in phylogenetic analysis. Mol. Biol. Evol. 17, 540-552.

Cramer, H. 1946. Mathematical methods of statistics. Princeton, Princeton University Press.

Dennis, A. B., Dunning, L. T., Sinclair, B. J., Buckley, T. R. 2015. Parallel molecular routes to cold adaptation in eight genera of New Zealand stick insects. Sci. Rep. 5, 13965.

Dowling, D., Friberg, U., Lindell, J., 2008. Evolutionary implications of non-neutral mitochondrial genetic variation. Trends Ecol. Evol. 23, 546–554.

Engel, M.S., Grimaldi, D.A., Krishna, K. 2007. Primitive termites from the Early Cretaceous. Stuttgarter Beitr Naturk. 371, 1–32.

Elbassiouny, A.A., Lovejoy, N.R., Chang, B.S.W., 2019. Convergent patterns of evolution of mitochondrial oxidative phosphorylation (OXPHOS) genes in electric fishes. Phil. Trans. R. Soc. B 375, 20190179–9.

Engel, M.S., Ortega-Blanco, J., Azar, D. 2011. The earliest earwigs in amber (Dermaptera): a new genus and species from the Early Cretaceous of Lebanon. Insect Syst. Evol. 42, 139–148.

Engel, M.S., Wang, B., Alqarni, A.S. 2016. A thorny, ‘anareolate’ stick-insect (Phasmatidae s.l.) in Upper Cretaceous amber from Myanmar, with remarks on diversification times among Phasmatodea. Cretac. Res. 63, 45–53.

Evangelista, D.A., Wipfler, B., Béthoux, O., Donath, A., Fujita, M., Kohli, M.K., et al. 2019. An integrative phylogenomic approach illuminates the evolutionary history of cockroaches and termites (Blattodea). Proc. Roy. Soc. B. 286, 20182076–20182079.

Foote, A.D., Morin, P.A., Durban, J.W., Pitman, R.L., Wade, P., Willerslev, E., Gilbert, M.T.P., da Fonseca, R.R. 2011. Positive selection on the killer whale mitogenome. Biol. Lett. 7, 116–118.

Forni, G., Puccio, G., Bourguignon, T., Evans, T., Mantovani, B., Rota-Stabelli, O., Luchetti A. 2019. Complete mitochondrial genomes from transcriptomes: assessing pros and cons of data mining for assembling new mitogenomes. Sci. Rep. 9, 14806.

Glaw, F., Hawlitschek, O., Dunz, A., Goldberg, J., Bradler, S., 2019. When giant stick insects play with colors: molecular phylogeny of the Achriopterini and description of

two new splendid species (Phasmatodea: Achrioptera) from Madagascar. Front. Ecol. Evol. 7, 125–18.

Goldberg, J., Bresseel, J., Constant, J., Kneubühler, B., Leubner, F., Michalik, P., Bradler, S. 2015. Extreme convergence in egg-laying strategy across insect orders. Sci. Rep. 5, 485–487.

Gorochov, A.V. 2013. New taxa of the superorder Orthopteroidea from the latter half of the Permian of European Russia. *Paleontol. J.* 47, 782-793.

Hassanin, A., Ropiquet, A., Couloux, A., Cruaud, C. 2009. Evolution of the mitochondrial genome in mammals living at high altitude: new insights from a study of the tribe Caprini (Bovidae, Antilopinae). J. Mol. Evol. 68, 293–310.

Huang, D.Y., Nel, A., Zompro, O., Waller, A. 2008. Mantophasmatodea now in the Jurassic. Naturwissenschaften. 95, 947–52.

Hughes, A.L. 2007. Looking for Darwin in all the wrong places: the misguided quest for positive selection at the nucleotide sequence level. Heredity, 99, 364–373.

Jiang, G.-F., 2018. Positive selection drove the adaptation of mitochondrial genes to the demands of flight and high-altitude environments in grasshoppers. Front. Genet. 9:605

Jordan, S.M.R., Barraclough, T.G., Rosindell, J. 2016. Quantifying the effects of the break up of Pangaea on global terrestrial diversification with neutral theory. Phil. Trans. R. Soc. B 371, 20150221–9.

Kalyaanamoorthy, S., Minh, B. Q., Wong, T. K., von Haeseler, A., Jermiin, L. S. 2017. ModelFinder: fast model selection for accurate phylogenetic estimates. Nat. Methods. 14, 587.

Katoh, K., Standley, D.M. 2013. MAFFT multiple sequence alignment software version 7: improvements in performance and usability. Mol. Biol. Evol. 30, 772–780.

Kobayashi, S., Usui, R., Nomoto, K., Ushirokita, M., Denda, T., Izawa, M., 2014. Does egg dispersal occur via the ocean in the stick insect *Megacrania tsudai* (Phasmida: Phasmatidae)? Ecol. Res. 29, 1025-1032.

Kômoto, N., Yukuhiro, K., Ueda, K., Tomita, S. 2011. Exploring the molecular phylogeny of phasmids with whole mitochondrial genome sequences. Mol. Phylogenet. Evol. 58, 43-52.

Kozak, K.M., Wahlberg, N., Neild, A.F.E., Dasmahapatra, K.K., Mallet, J., Jiggins, C.D. 2015. Multilocus species trees show the recent adaptive radiation of the mimetic *Heliconius* butterflies. Syst. Biol. 64, 505–24.

Krishna, K., Grimaldi, D.A., Krishna, V., Engel, M.S., 2013. Treatise on the Isoptera of the World: volume 1 Introduction. Bull. Am. Mus. Nat. Hist. 377, 1–200.

Lanfear, R., Frandsen, P.B., Wright, A.M., Senfeld, T., Calcott, B. 2016. PartitionFinder 2: new methods for selecting partitioned models of evolution for molecular and morphological phylogenetic analyses. Mol. Biol. Evol. 34, 772–773.

Larsson, A. 2014. AliView: a fast and lightweight alignment viewer and editor for large datasets. Bioinformatics. 30, 3276-3278.

Legendre, F., Nel, A., Svenson, G. J., Robillard, T., Pellens, R., Grandcolas, P. 2015. Phylogeny of Dictyoptera: dating the origin of cockroaches, praying mantises and termites with molecular data and controlled fossil evidence. PloS ONE. 10, e0130127.

Li, H. et al., 2017. Mitochondrial phylogenomics of Hemiptera reveals adaptive innovations driving the diversification of true bugs. Proc. R. Soc. B. 284, 20171223.

López-Estrada, E.K., Sanmartín, I., García-París, M., Zaldívar-Riverón, A. 2018. High extinction rates and non-adaptive radiation explains patterns of low diversity and extreme morphological disparity in North American blister beetles (Coleoptera, Meloidae). Mol. Phylogenet. Evol.130, 156–68.

Matschiner, M., Hanel, R., Salzburger, W. 2011. On the origin and trigger of the notothenioid adaptive radiation. PloS ONE. 6, e18911.

McIntyre, S.R.N., Lineweaver, C.H., Groves, C.P., Chopra, A. 2017. Global biogeography since Pangaea. Proc. R. Soc. B. 284, 20170716.

Misof, B., Liu, S., Meusemann, K., Peters, R.S., Donath, A., Mayer, C., et al. 2014. Phylogenomics resolves the timing and pattern of insect evolution. Science. 346, 763-767.

Montagna, M., Tong, K.J., Magoga, G., Strada, L., Tintori, A., Ho, S.Y.W., Lo, N., 2019. Recalibration of the insect evolutionary time scale using Monte San Giorgio fossils suggests survival of key lineages through the End-Permian Extinction. Proc. Roy. Soc. B 286, 20191854–20191859.

Ohta T., 1993. Amino acid substitution at the *Adh* locus of Drosophila is facilitated by small population size. Proc Natl Acad Sci USA, 90, 4548-4551.

Plazzi, F., Puccio, G., Passamonti, M., 2017. Burrowers from the past: mitochondrial signatures of Ordovician bivalve infaunalization. Genome Biol. Evol. 9, 956–967.

Rambaut, A., Drummond, A.J., Xie, D., Baele, G., Suchard, M.A. 2018. Posterior summarisation in Bayesian phylogenetics using Tracer 1.7. Syst. Biol. 67, 901-904.

Robertson, J.A., Bradler, S., Whiting, M.F. 2018. Evolution of oviposition techniques in stick and leaf insects (Phasmatodea). Front. Ecol. Evol. 6, 125–15.

Roelants, K., Gower, D.J., Wilkinson, M., Loader, S.P., Biju, S.D., Guillaume, K., Moriau, L., Bossuyt, F. 2007. Global patterns of diversification in the history of modern amphibians. Proc. Natl. Acad. Sci. USA 104, 887–892.

Rota-Stabelli, O., Telford, M.J. 2008. A multi criterion approach for the selection of optimal outgroups in phylogeny: recovering some support for Mandibulata over Myriochelata using mitogenomics. Mol. Phylogenet. Evol. 48,103–111.

Rutschmann, S., Chen, P., Zhou, C., Monaghan, M.T. 2017. Using mitochondrial genomes to infer phylogenetic relationships among the oldest extant winged insects (Palaeoptera). BioRxiv 1–33, https://doi.org/10.1101/164459

Sharov, A.G., 1961. Otryad Plecoptera (Order Plecoptera). Paleozojskoe nasekomye Kuznetskovo bassejna [Paleozoic insects from the Kuznetsk basin]. Tr. Paleontol. Inst. Akad. Nauk SSSR 85, 225–234.

Suetsugu, K., Funaki, S., Takahashi, A., Ito, K., Yokoyama, T. 2018. Potential role of bird predation in the dispersal of otherwise flightless stick insects. Ecology. 99, 1504–1506.

Shen, Y.Y., Liang, L., Zhu, Z.H., Zhou, W.P., Irwin, D.M., Zhang, Y.P. 2010. Adaptive evolution of energy metabolism genes and the origin of flight in bats. Proc. Natl. Acad. Sci. USA. 107, 8666-8671.

Simões, M., Breitkreuz, L., Alvarado, M., Baca, S., Cooper, J.C., Heins, L., Lieberman, B.S., 2016. The evolving theory of evolutionary radiations. Trends Ecol. Evol. 31, 27-34.

Simon, S., Letsch, H., Bank, S., Buckley, T.R., Donath, A., Liu, S., Machida, R., Meusemann, K., Misof, B., Podsiadlowski, L., Zhou, X., Wipfler, B., Bradler, S., 2019. Old World and New World Phasmatodea: phylogenomics resolve the evolutionary history of stick and leaf insects. Front. Ecol. Evol. 7, 744–14.

Song, H., Amédégnato, C., Cigliano, M.M., Desutter-Grandcolas, L., Heads, S.W., Huang, Y., et al. 2015. 300 million years of diversification: elucidating the patterns of orthopteran evolution based on comprehensive taxon and gene sampling. Cladistics. 31, 621–651.

Svenson, G.J., Whiting, M.F. 2009. Reconstructing the origins of praying mantises (Dictyoptera, Mantodea): the roles of Gondwanan vicariance and morphological convergence. Cladistics. 25, 468–514.

Tang, P., Zhu, J.C., Zheng, B.Y., Wei, S.J., Sharkey, M., Chen, X.X., et al. 2019. Mitochondrial phylogenomics of the Hymenoptera. Mol. Phylogenet. Evol. 131, 8–18.

Tilgner, E.H., 2002. Systematics of phasmida, Unpublished PhD. Thesis. University of Georgia.

Timmermans, M.J.T.N., Lees, D.C., Simonsen, T.J. 2014. Towards a mitogenomic phylogeny of Lepidoptera. Mol. Phylogenet. Evol. 79, 169–78.

Toljagic, O., Butler, R. J., 2013. Triassic-Jurassic mass extinction as trigger for the Mesozoic radiation of crocodylomorphs. Biol. Lett. 9, 20130095–20130095.

Tomasco, I.H., Lessa, E.P. 2011. The evolution of mitochondrial genomes in subterranean caviomorph rodents: adaptation against a background of purifying selection. Mol. Phylogenet. Evol. 61, 64–70.

Tong, K.J., Duchene, S., Ho, S.Y.W., Lo, N., 2015. Comment on “Phylogenomics resolves the timing and pattern of insect evolution”. Science. 349, 487-487.

Trewick, S.A., Morgan-Richards M., Collins J.L. 2008. Are you my mother? Phylogenetic analysis reveals orphan hybrid stick insect genus is part of a monophyletic New Zealand clade. Mol. Phylogenet. Evol. 48, 799-808.

Trifinopoulos, J., Nguyen, L.T., von Haeseler, A., Minh, B. Q. 2016. W-IQ-TREE: a fast online phylogenetic tool for maximum likelihood analysis. Nucl. Acids Res. 44(W1), W232-W235.

Vickery, V. R., Sandoval, C. P. 2001. Descriptions of three new species of *Timema* (Phasmatoptera: Timematodea: Timematidae) and notes on three other species. J Orthoptera Res. 10(1), 53-61.

Villanueva-Cañas, J. L., Laurie, S., Albà, M. M. 2013. Improving genome-wide scans of positive selection by using protein isoforms of similar length. *Genome Biol Evol*. *5*(2), 457–467.

Vrba, E. S., 1993. Turnover-pulses, the Red Queen, and related topics. Am. J. Sci. 293, 418.

Vrsansky, P., 2002. Origin and the early evolution of mantises. Amba Proj. 6, 1-16.

Wang, Y., Shen, Y., Feng, C., Zhao, K., Song, Z., Zhang, Y., Yang, L., He, S. 2016. Mitogenomic perspectives on the origin of Tibetan loaches and their adaptation to high altitude. Sci. Rep. 6, 2969.

Wedmann, S., Bradler, S., Rust, J., 2007. The first fossil leaf insect: 47 million years of specialized cryptic morphology and behavior. Proc. Natl. Acad. Sci. USA. 104, 565–569.

Whitfield, J.B., Lockhart, P.J. 2007. Deciphering ancient rapid radiations. Trends Ecol. Evol. 22, 258–265.

Whiting, M. F., Bradler, S., Maxwell, T., 2003. Loss and recovery of wings in stick insects. Nature. 421, 264.

Wolfe, J.M., Daley, A.C., Legg, D.A., Edgecombe, G.D. 2016. Fossil calibrations for the arthropod Tree of Life. Earth Sci. Rev. 160, 43–110.

Woolfit, M., Bromham, L. 2005. Population size and molecular evolution on islands. Proc Biol Sci, 272(1578), 2277-2282.

Xia X. 2018. DAMBE7: New and improved tools for data analysis in molecular biology and evolution. Mol. Biol. Evol. 35, 1550–1552

Yang, Z. 2007. PAML 4: Phylogenetic Analysis by Maximum Likelihood. Mol. Biol. Evol. 24, 1586-1591.

Yang H, Yin X, Lin X, Wang C, Shih C, Zhang W, Ren D, Gao T., 2019. Cretaceous winged stick insects clarify the early evolution of Phasmatodea. Proc. Biol. Sci. 286(1909), 20191085.

Yuan, M.L., Zhang, Q.-L., Zhang, L., Jia, C.L., Li, X.P., Yang, X.Z., et al. 2018. Mitochondrial phylogeny, divergence history and high-altitude adaptation of

grassland caterpillars (Lepidoptera Lymantriinae Gynaephora) inhabiting the Tibetan Plateau. Mol. Phylogenet. Evol. 122, 116–24.

Zhou, T., Shen, X., Irwin, D.M., Shen, Y., Zhang, Y., 2014. Mitogenomic analyses propose positive selection in mitochondrial genes for high-altitude adaptation in galliform birds. Mitochondrion. 18, 70–75.

Zhou, Z., Guan, B., Chai, J., Che, X. 2017. Next-generation sequencing data used to determine the mitochondrial genomes and a preliminary phylogeny of Verophasmatodea insects. J. Asia-Pac. Entomol. 20, 713-719.

Legend for figures:

Figure 1 – Maximum likelihood tree obtained from the full dataset, with pictures illustrating some of the stick and leaf insects analysed in the present paper.

Figure 2 – Bayesian phylogeny and estimates of divergence time for Phasmatodea lineages. Asterisks highlight newly assembled mitogenomes; the scale on the top indicates Million years.

Figure 3 – Comparison of divergence dates of Euphasmatodean stem (blue) and crown (yellow) nodes relatively to (a) variation in median dN/dS values thourgh time and (b) to three-timer (3T) origination and extinction rates of arthropods obtained by the Fossilworks portal.

Figure S1 – Outcome of the AliGROOVE analysis, including and excluding 3rd codon position.

Figure S2 - A: ML inference on the nucleotide dataset (13 PCGs with third codon position excluded and 2 rRNA). B: ML inference on the amino acid dataset (13 PCGs). C: Estimate of divergence on the nucleotide dataset (13 PCGs with third codon position excluded and 2 rRNA) using a yule tree prior. D: Estimate of divergence time on the nucleotide dataset (13 PCGs with third codon position excluded and 2 rRNA) using a Birth-Death tree prior. For A-D: posterior probabilities and rapid bootstrap values are reported at nodes only if they are < 1 and < 100 respectively. For C - D: calibration points described in Table 2 are marked in red with the letters from A to L. E: ML inference on the amino acid dataset (left panel, 13 PCGs) and on the nucleotide dataset (right panel, 13 PCGs with third codon position excluded and 2 rRNA).

Figure S3 - Plot of median values of dN, dS and dN/dS through time and their linear regression with time for each PCG of the mitochondrion and their concatenation for the whole dataset (A) and phasmatodea only (B). In the C panel, the plot of median values of

dN, dS and dN/dS against branch length and their linear regression. In the D panel dN/dS ratios were plotted against corresponding dS values in both complete dataset (left) and in Phasmatodea only (right)

Figure S4 – Comparison of the dating of the main polyneopteran lineages with relevant literature.

Figure 1

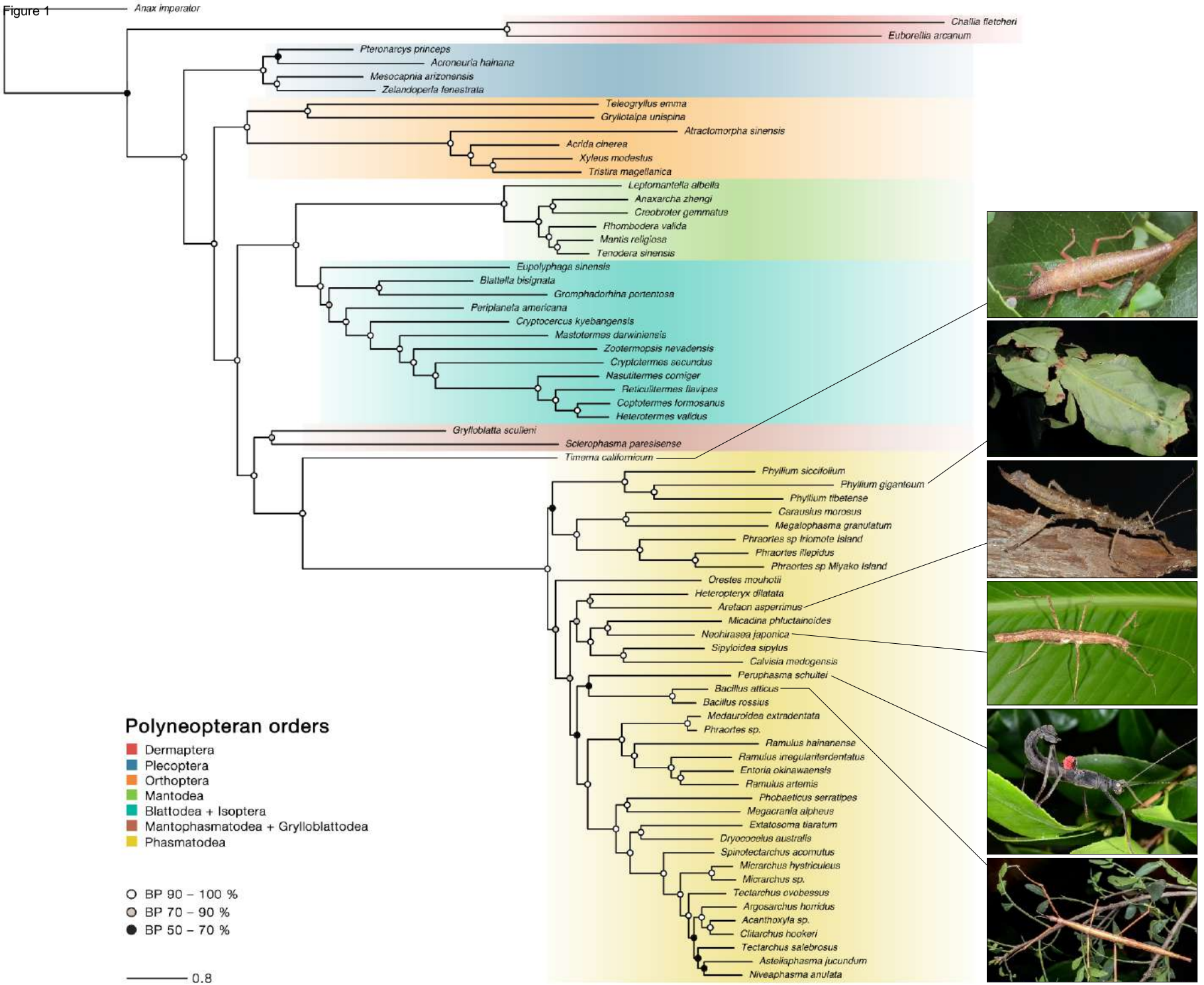
Anax imperator
Challia fletcheri
Euborellia arcanum
Pteronarcys princeps
Acroneuria hainana
Mesocapnia arizonensis
Zelandoperla fenestrata
Teleogryllus emma
Gryllotalpa unispina
Atractomorpha sinensis
Acrida cinerea
Xyleus modestus
Tristira magellanica
Leptomantella albella
Anaxarcha zhengi
Creobroter gemmatus
Rhombodera valida
Mantis religiosa
Tenodera sinensis
Eupolyphaga sinensis
Blattella bisignata
Gromphadorhina portentosa
Periplaneta americana
Cryptocercus kyebangensis
Mastotermes darwiniensis
Zootermopsis nevadensis
Cryptotermes secundus
Nasutitermes corniger
Reticulitermes flavipes
Coptotermes formosanus
Heterotermes validus
Grylloblatta sculleni
Sclerophasma paresisense
Timema californicum
Phyllium siccifolium
Phyllium giganteum
Phyllium tibetense
Carausius morosus
Megalophasma granulatum
Phraortes sp Iriomote island
Phraortes illepidus
Phraortes sp Miyako Island
Orestes mouhotii
Heteropteryx dilatata
Aretaon asperrimus
Micadina phluctainoides
Neohirasea japonica
Sipyloidea sipylus
Calvisia medogensis
Peruphasma schultei
Bacillus atticus
Bacillus rossius
Medauroidea extradentata
Phraortes sp.
Ramulus hainanense
Ramulus irregulariferdentatus
Entoria okinawaensis
Ramulus artemis
Phobaeticus serratipes
Megacrania alpheus
Extatosoma tiaratum
Dryococelus australis
Spinotectarchus acomutus
Micrarchus hystriculeus
Micrarchus sp.
Tectarchus ovobessus
Argosarchus horridus
Acanthoxyla sp.
Clitarchus hookeri
Tectarchus salebrosus
Asteliaphasma jucundum
Niveaphasma anulata
Polyneopteran orders
Dermaptera
Plecoptera
Orthoptera
Mantodea
Blattodea + Isoptera
Mantophasmatodea + Grylloblattodea
Phasmatodea
BP 90 – 100 %
BP 70 – 90 %
BP 50 – 70 %
0.8

Figure 2

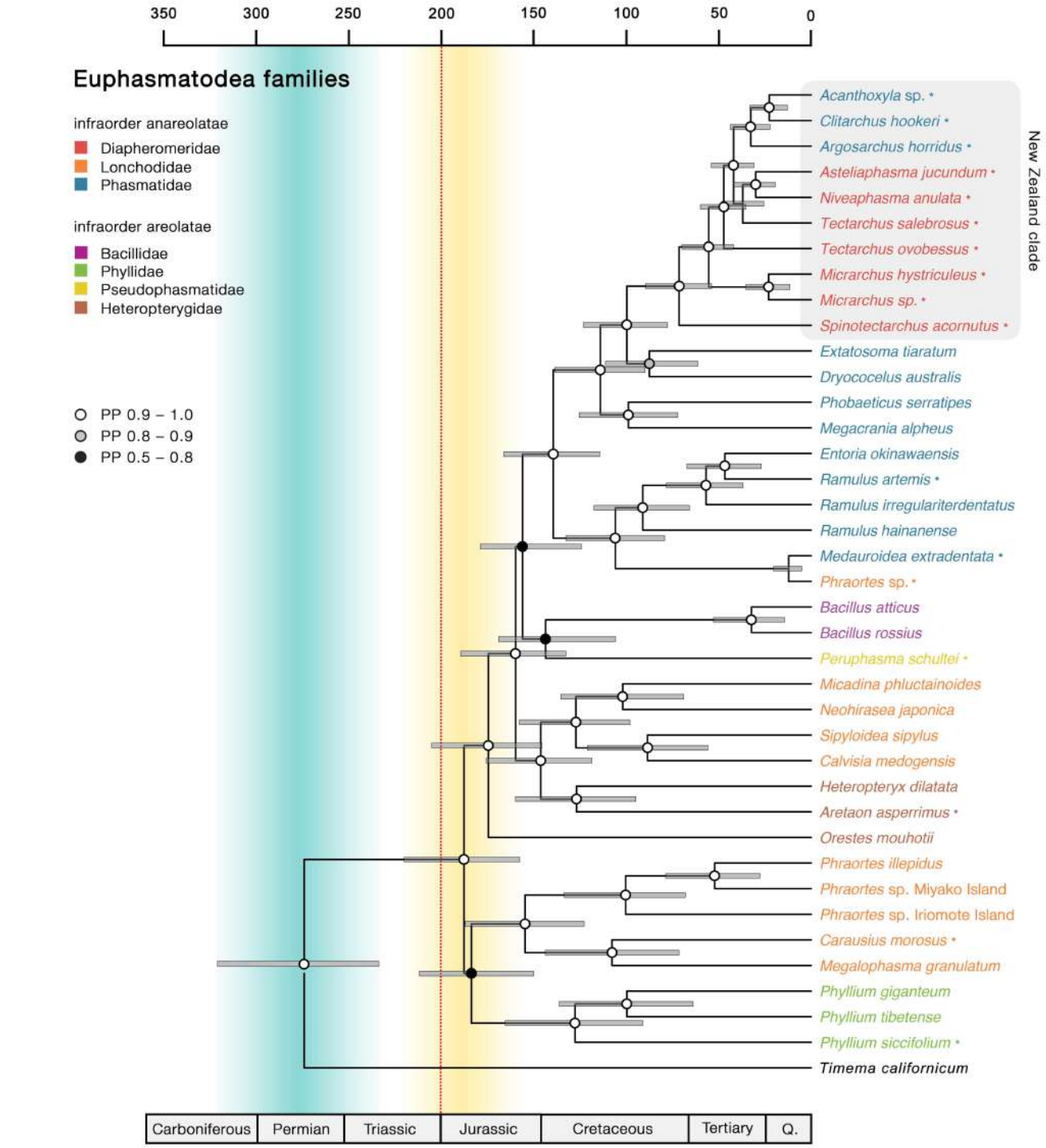
350
300
250
200
150
100
50
0
Euphasmatodea families
infraorder anareolatae
Diapheromeridae
Lonchodidae
Phasmatidae
infraorder areolatae
Bacillidae
Phyllidae
Pseudophasmatidae
Heteropterygidae
PP 0.9 – 1.0
PP 0.8 – 0.9
PP 0.5 – 0.8
New Zealand clade
Acanthoxyla sp.
Clitarchus hookeri
Argosarchus horridus
Asteliaphasma jucundum
Niveaphasma anulata
Tectarchus salebrosus
Tectarchus ovobessus
Micrarchus hystriculeus
Micrarchus sp.
Spinotectarchus acornutus
Extatosoma tiaratum
Dryococelus australis
Phobaeticus serratipes
Megacrania alpheus
Entoria okinawaensis
Ramulus artemis
Ramulus irregulariterdentatus
Ramulus hainanense
Medauroidea extradentata
Phraortes sp.
Bacillus atticus
Bacillus rossius
Peruphasma schultei
Micadina phluctainoides
Neohirasea japonica
Sipyloidea sipylus
Calvisia medogensis
Heteropteryx dilatata
Aretaon asperrimus
Orestes mouhotii
Phraortes illepidus
Phraortes sp. Miyako Island
Phraortes sp. Iriomote Island
Carausius morosus
Megalophasma granulatum
Phyllium giganteum
Phyllium tibetense
Phyllium siccifolium
Timema californicum
Carboniferous
Permian
Triassic
Jurassic
Cretaceous
Tertiary
Q.

Figure 3

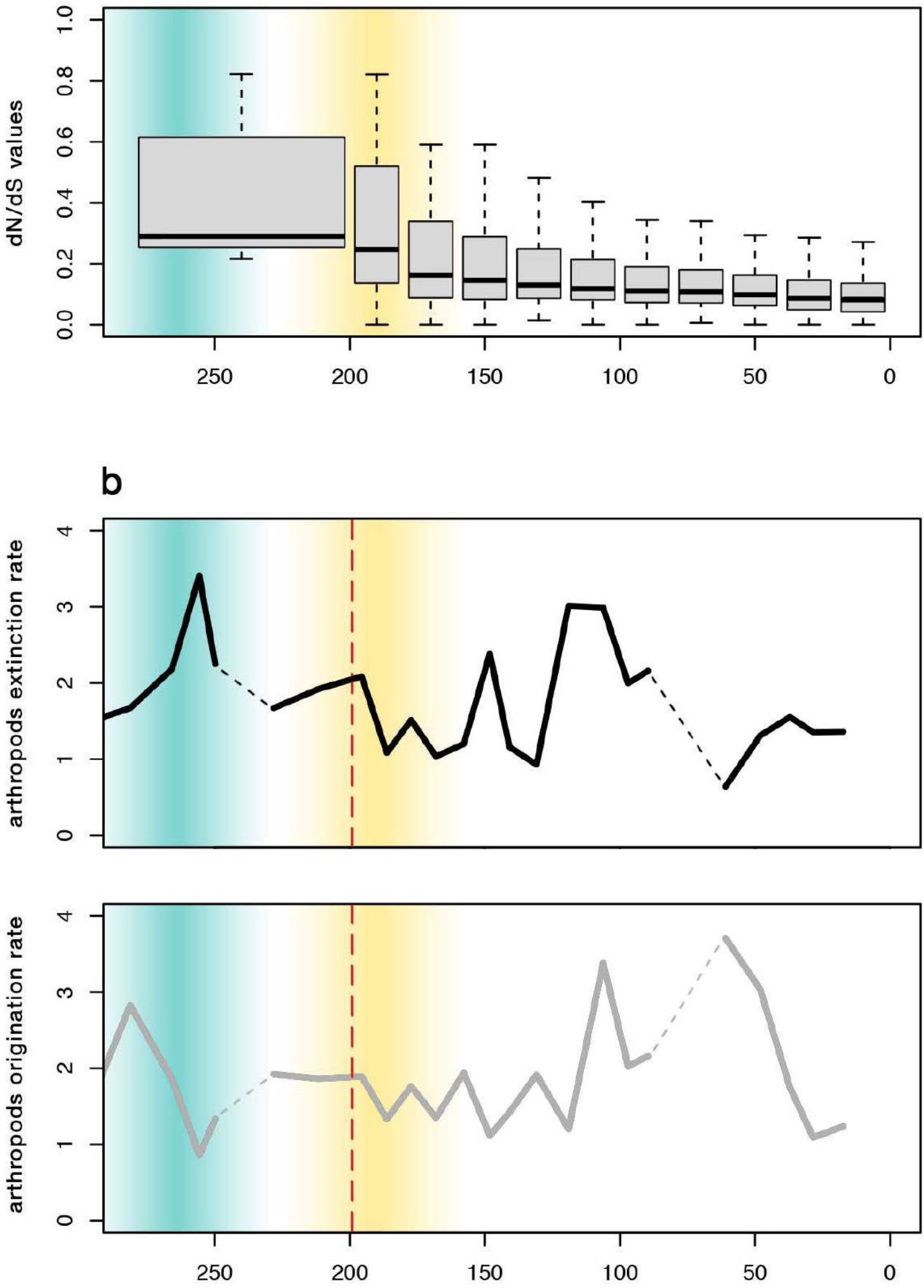
a
dN/dS values
0.0
0.2
0.4
0.6
0.8
1.0
250
200
150
100
50
0
b
arthropods extinction rate
0
1
2
3
4
arthropods origination rate
0
1
2
3
4
250
200
150
100
50
0

Table 1

Genbank accession numbers for the 17 RNA-Seq experiments and the 21 assembled mitogenomes utilized.

Species	**Genbank acc. no.**	**SRA**
Acanthoxyla sp.		SRR2089887
Aretaon asperrimus		SRR1172270
Argosarchus horridus		SRR2089902
Asteliaphasma jucundum		SRR2089913
Carausius morosus		SRR3211828
Clitarchus hookeri		SRR3080266
Medauroidea extradentata		SRR1172394
Micrarchus sp.		SRR1054193
Micrarchus hystriculeus		SRR1054191
Niveaphasma anulata		SRR2089878
Peruphasma schultei		SRR1002984
Phraortes sp. YW-2014		SRR1189755
Phyllium siccifolium		ERR392012
Ramulus artemis		SRR1172422
Spinotectarchus acornutus		SRR2089897
Tectarchus salebrosus		SRR2089908
Tectarchus ovobessus		SRR2089893
Bacillus atticus	GU001955	
Bacillus rossius	GU001956	
Calvisia medogensis	KY124330	
Dryococelus australis	AP018522	
Extatosoma tiaratum	AB642680	
Entoria okinawaensis	AB477459	
Heteropteryx dilatata	AB477468	
Megacrania alpheus	AB477471	
Megalophasma granulatum	KY124331	
Micadina phluctainoides	AB477466	
Neohirasea japonica	AB477469	
Orestes mouhotii	AB477462	
Phobaeticus serratipes	AB477467	
Phraortes illepidus	AB477460	
Phraortes sp. Iriomote Island	AB477464	
Phraortes sp. Miyako Island	AB477465	
Phyllium giganteum	AB477461	
Phyllium tibetense	KY124332	
Ramulus irregulariterdentatus	AB477463	
Ramulus hainanense	FJ156750	
Sipyloidea sipylus	AB477470	
Timema californicum	DQ241799	

Table 2
Fossil records, dating and calibration points for the divergence time analysis.

Species	Minimum age (Mya)	Maximum age (Mya)	Calibration group	Reference
Rhadinolabis phoenicica	129.4	411	crown Dermaptera	Engel et al., 2011
Palaeotaeniopteryx elegans	268.3	411	crown Plecoptera	Sharov et al., 1961
Oedischia williamsoni	299.0	411	stem Orthoptera	Brongniart et al., 1885
Raphogla rubra	271.8	411	crown Orthoptera	Bethoux et al., 2002
Juramantis initialis	145	316	crown Dyctioptera	Vrsansky et al., 2002
Valditermes brennenae	130.3	325	crown Isoptera	Krishna et al., 2013
Reticulitermes antiquus	33.9	95	crown Coptotermitinae + Heterotermitinae	Engel et al., 2007
Juramantophasma sinica	158.1	411	stem Mantophasmatodea - Grylloblattodea	Huang et al., 2008
Echinosomiscus primoticus	98.2	411	crown Phasmatodea	Engel et al., 2016
Eophyllium messelensis	47.0	411	stem *Phyllium*	Wedeman et al., 2007

Table 3
Values of dN/dS. dN and dS obtained for *T. californicum* and Euphasmatodea stem branches

	ATP6	ATP8	CO1	CO2	CO3	CYTB	ND1	ND2	ND3	ND4	ND4L	ND5	ND6	Concatenated
T. californicum dN/dS	0.099	0.481	0.043	0.085	0.089	0.063	0.107	0.188	0.217	0.106	0.110	0.094	0.262	0.113
T. californicum dN	0.034	0.064	0.017	0.031	0.029	0.024	0.042	0.047	0.050	0.039	0.042	0.038	0.055	0.036
T. californicum dS	0.341	0.132	0.389	0.361	0.329	0.373	0.390	0.248	0.231	0.372	0.383	0.409	0.210	0.319
Euphasmatodea dN/dS	0.285	NA	0.216	0.263	0.770	0.267	0.246	0.497	0.295	0.246	0.821	0.443	0.731	0.546
Euphasmatodea dN	0.052	0.075	0.044	0.051	0.065	0.049	0.054	0.060	0.053	0.053	0.066	0.061	0.065	0.061
Euphasmatodea dS	0.183	0.000	0.205	0.192	0.084	0.185	0.219	0.121	0.181	0.214	0.081	0.137	0.089	0.112
Fold change	2.9	NA	5.1	3.1	8.6	4.2	2.3	2.6	1.4	2.3	7.4	4.7	2.8	4.8

Giobbe Forni, Andrea Luchetti: Conceptualization, Investigation, Writing- Original draft preparation, Writing- Reviewing and Editing. **Giobbe Forni, Federico Plazzi**: Data curation, Software, Formal analysis. **Oskar Conle, Franck Henneman**: Validation, Writing- Original draft preparation **Andrea Luchetti, Barbara Mantovani:** Supervision, Funding acquisition.